European Journal of Pharmaceutical Sciences 169 (2022) 106097

Contents lists available at ScienceDirect

European Journal of Pharmaceutical Sciences

journal homepage: www.elsevier.com/locate/ejps

Oral administration of buparvaquone nanostructured lipid carrier enables *in vivo* activity against *Leishmania infantum*

Lis Marie Monteiro [a], Raimar Löbenberg [b], Eduardo José Barbosa [a,*], Gabriel Lima Barros de Araujo [a], Paula Keiko Sato [c], Edite Kanashiro [c,d], Raissa H. de Araujo Eliodoro [c], Mussya Rocha [c], Vera Lúcia Teixeira de Freitas [c], Nikoletta Fotaki [e], Nádia Araci Bou-Chacra [a,*]

[a] Department of Pharmacy, Faculty of Pharmaceutical Sciences, University of São Paulo, Professor Lineu Prestes Av, 580, Cidade Universitária, 05508-000 São Paulo, SP, Brazil
[b] Faculty of Pharmacy and Pharmaceutical Sciences, University of Alberta, 8613 - 114St NW, T6G 2H7, Edmonton, AB, Canada
[c] Laboratory of Medical Investigation in Immunology (LIM48), Hospital das Clínicas, Faculdade de Medicina FMUSP, Universidade de São Paulo, Av. Dr. Eneas Carvalho de Aguiar, 470, IMT2, térreo, 05403-000, São Paulo, SP, Brazil
[d] Seroepidemiology, Cellular, and Molecular Immunology Laboratory - Institute of Tropical Medicine, University of São Paulo, Dr. Enéas de Carvalho Aguiar, 470 - Jardim América, São Paulo, SP, 05403-000, Brazil
[e] Department of Pharmacy & Pharmacology, University of Bath, Claverton Down, Bath, BA2 7AY, United Kingdom

ARTICLE INFO

Keywords:
Buparvaquone
Nanostructured lipid carrier
Leishmaniasis
Neglected diseases

ABSTRACT

Leishmaniasis, a neglected tropical disease, is prevalent in 98 countries with the occurrence of 1.3 million new cases annually. The conventional therapy for visceral leishmaniasis requires hospitalization due to the severe adverse effects of the drugs, which are administered parenterally. Buparvaquone (BPQ) showed *in vitro* activity against leishmania parasites; nevertheless, it has failed *in vivo* tests due to its low aqueous solubility. Though, lipid nanoparticles can overcome this holdback. In this study we tested the hypothesis whether BPQ-NLC shows *in vivo* activity against L. *infantum*. Two optimized formulations were prepared (V1: 173.9 ± 1.6 nm, 0.5 mg of BPQ/mL; V2: 232.4 ± 1.6 nm, 1.3 mg of BPQ/mL), both showed increased solubility up to 73.00-fold, and dissolution up to 83.29%, while for the free drug it was only 2.89%. Cytotoxicity test showed their biocompatibility (CC50 >554.4 μM). Besides, the V1 dose of 0.3 mg/kg/day for 10 days reduced the parasite burden in 83.4% ±18.2% (p <0.05) in the liver. BPQ-NLC showed similar leishmanicidal activity compared to miltefosine. Therefore, BPQ-NLC is a promising addition to the limited therapeutic arsenal suitable for leishmaniasis oral administration treatment.

1. Introduction

Leishmaniases are among the leading neglected tropical diseases (NTDs). New cases occur worldwide from 1.5 to 2 million per year. They are highly associated with poverty and prevalent in 89 countries, in four of the five continents. More than 1 billion people are living in endemic areas, and the estimated number of deaths from visceral leishmaniases ranges from 20,000 to 70,000 per year (HEALTH, W. ORGANIZATION 2017).

As an obligate intracellular parasite, leishmania is shielded from conventional chemotherapy, which does not readily diffuse through the host cellular membrane. The pentavalent antimonial drugs such as meglumine antimoniate or sodium stibogluconate have been the first-line treatment for more than 60 years, with a success rate between 60 and 80%. Moreover, the therapy for visceral leishmaniasis requires hospitalization to monitor severe adverse effects due to the parenteral administration of large and repeated doses, which can last from 20 to 40 days. Additionally, resistance to second-line drugs, such as miltefosine and liposomal amphotericin B, is prone to develop (Burza et al., 2018; Costa Lima et al., 2012).

Aiming to discover new drugs, a series of hydroxynaphthoquinones were synthetized in the 1980s. Considering the potential of these molecules for use in the treatment of neglected diseases, they were tested *in vitro* against *Leishmania donovani*. Buparvaquone (BPQ) showed 100-fold

* Corresponding authors.
E-mail addresses: eduardo.jose.barbosa@usp.br (E.J. Barbosa), chacra@usp.br (N.A. Bou-Chacra).

https://doi.org/10.1016/j.ejps.2021.106097
Received 17 April 2021; Received in revised form 9 December 2021; Accepted 10 December 2021
Available online 12 December 2021

increased activity against amastigotes (intracellular parasite form) compared to other hydroxynaphthoquinones (Croft et al., 1992; Vexenat et al., 1998). However, in dogs infected with L. *(L.) infantum*, only a negligible effect was observed. The aqueous solubility of BPQ is very low (<1 mg.L^{-1}), and therefore it is poorly soluble in biological fluids, such as gastric and interstitial juices. In addition to the low water solubility, drug CYP metabolism by liver enzymes may also explain the drug's low bioavailability and limited *in vivo* efficacy (Smith et al., 2018).

Approximately 80% of drugs are preferentially administered by the oral route. The most evident benefits include ease of administration, cost-effective manufacturing, less rigid storage conditions, high patient compliance, and more accurate self-administered dose. However, a drug substance must have proper absorption from the gastrointestinal tract (GIT). Stability in the gastric environment and aqueous solubility at GIT pH are imperative for the development of an oral dosage form (Date et al., 2019; Tran et al., 2019).

The development of nanostructured delivery systems is one of the most promising alternatives to conventional treatments in meeting the leishmaniases therapy needs (de Souza et al., 2021). The advantages of nanostructured systems comprise the enhancement of water solubility of poorly water-soluble drugs, and the development of modified and site-specific drug delivery systems, which have the potential to increase the therapeutic efficacy and reduce drug toxicity (Korani et al., 2019; Kobets et al., 2012). Among the options, nanostructured lipid carriers (NLC), composed of biocompatible lipids, have attracted the attention of formulation scientists as carriers for the modified release of poorly water-soluble drugs (Gordillo-Galeano and Mora-Huertas, 2018; Das et al., 2012). These carriers have been introduced as alternatives to conventional colloidal ones, such as liposomes and polymeric nanoparticles, due to improved physical and chemical stability, the viability of industrial scale and lower cost of raw materials (Alavi and Hamidi, 2019; Souto et al., 2020). Also nanostructured lipids have the potential to reduce drug degradation by liver, owing to selective lymphatic absorption (Shrivastava et al., 2020).

Hence, considering the potential of nanotechnology-based drug delivery systems and the need for an innovative product to treat leishmaniasis, we tested the hypothesis whether oral administration of affordable and safe BPQ nanostructured lipid carrier presents suitable *in vivo* activity against *Leishmania infantum*. The formulations were developed and optimized using design of experiments (DoE), taking into consideration the factors with high impact over the product quality profile. To the best of our knowledge, this study is the first one to show a proof of concept and *in vitro* immunomodulatory effects of BPQ-NLC for the treatment of leishmaniasis.

2. Materials and methods

2.1. Materials

Softisan® 154 was kindly donated by CREMER Oleo Division (Germany), glyceryl monocaprylate, medium-chain triglycerides (MCT) were kindly donated by Abitec (USA). Kolliphor® P188 was acquired from BASF (Germany) and Tween 80 from Millipore Sigma (Germany). Buparvaquone (purity 99.5%) was donated by Shaanxi King Stone (Xian, China). Buparvaquone analytical standard Vetranal Supelco was purchased from Merck Sigma (Germany). Culture media M199 and RPMI 1640, and MTT reagent (3-(4,5-dimethylthiazol-2-yl)−2,5-diphenyl tetrazolium bromide) were purchased from Merck Sigma (Germany). Pancreatin (*4X USP activity)* was purchased from Merck Sigma (Germany). Purified water was obtained by a Milli-Q system from Merck Millipore (Germany). Organic solvents were HPLC grade, and all other chemicals used were of the at least analytical grade.

2.2. Development of BPQ-NLC

Lipids were selected as described in our previous work (L.M. Monteiro et al., 2017). The buparvaquone nanostructured lipid carrier (BPQ-NLC) formulations were prepared by dissolving free BPQ into the melted lipid phase for 15 min. The aqueous phase (70 °C) was added to the lipid phase and mixed for 5 min. The BPQ encapsulation efficiency was 99% of the amount added in the beginning of the process. Pre-homogenization was performed using a high-performance disperser (8000 RPM for 5 min) (T25 digital ULTRA-TURRAX, IKA, Staufen, Germany). Afterward, the emulsion was passed through a high-pressure homogenizer (Nano DeBEE 45–2, Bee International, South Easton, MA, USA) at 600 bars for five cycles. The solid lipid, liquid lipid, and the surfactant were Softisan 154, MCT (capric/caprylic triglyceride) (1:2), and poloxamer 188, respectively.

Factors with high risk or impact over the quality of preparations were selected: liquid and solid lipid ratio, surfactant concentration, and lipid phase amount. A full factorial 2^3 design (Table 1) was carried out to evaluate the influence of the factors in Z-average. The preparations were performed in random order to minimize systematic error. Statistical analysis was performed ($\alpha = 0.05$) using Minitab 19 (Stage College, Pennsylvania). The high performance liquid chromatography (HPLC) method (supplementary data) was described in our previous work to quantify BPQ in NLC (L.M. Monteiro et al., 2017).

2.3. Determination of the Z-average, polydispersity index, and zeta potential

The Z-average, polydispersity index (PDI), particle size distribution, and zeta potential of BPQ-NLC were determined immediately after homogenization and periodically for the stability study (supplementary data). The method used was photon correlation spectroscopy (PCS) using Zetasizer Nano ZS90 (Malvern Instruments, Malvern, UK) at 25 °C and 90 °C angle ($n = 10$). The measurements were carried out in purified water ($n = 3$), with conductivity adjusted to 50 μS.cm^{-1} by the addition of NaCl 0.1% w/w, aiming to avoid fluctuations in ZP. The pH was adjusted to 6.5 ± 0.2 by the addition of 0.01 M HCl or 0.01 M NaOH solution.

2.4. Drug loading and entrapment efficiency

Drug loading (DL) and entrapment efficiency (EE%) were determined after homogenization and periodically during the stability study (supplementary data) by the HPLC method cited in Section 2.2. For DL, the amount of BPQ (mg) in 1 mL of preparation was determined as follows: aliquots were diluted to a volumetric flask to a final BPQ concentration of 0.005 mg.mL^{-1} and the volume was filled with the mobile phase. The previous preparations were filtered with PVDF membrane, 0.45 μM pore size (MilliporeSigma, Germany). Each BPQ-NLC preparation was evaluated in triplicate. The drug load was previously evaluated, and the lipid matrix could accommodate 1% of drug by weight.

EE (%) of BPQ-NLCs was calculated by determining the amount of free drug using ultrafiltration technique. The free BPQ (mg) in 1 mL of preparation was determined as follows: an aliquot of each formulation was placed in EMD Millipore Amicon™ centrifuge filter units, 100 Kd MWCO (MilliporeSigma, Germany). The samples were centrifuged 14,000 g at 20 °C for 30 min. The BPQ-NLCs were evaluated in triplicate. EE was calculated using Eq. (1) and DL using Eq. (2):

$$\%EE = (Wtotal - Wfree)/(Wtotal)\ x\ 100 \quad (1)$$

Table 1
Formulation design space of buparvaquone nanostructured lipid carrier. Low and high levels determined by preliminary tests.

Factor	Abbreviation	Low level	High level
The ratio of solid and liquid lipids	SL:LL	0.5	3.0
Poloxamer 188 (% w/w)	% POL	1.0	4.0
Lipid phase (% w/w)	% LP	5.0	15.0

$$DL\% = (Wtotal - Wfree)/(Wlipid)\ x\ 100 \quad (2)$$

where W_{total} is the weight of initial BPQ added, W_{free} is the weight of free drug detected in the filtrate after centrifugation, and W_{lipid} is the weight of lipid at the formulation.

2.5. Morphology by transmission electron microscopy (TEM)

BPQ-NLCs images were acquired using a Morgagni 268 transmission electron microscope with Gatan Digital Camera (Philips/FEI, Hillsboro, Oregon, USA). The samples were diluted in purified water in the ratio of 1:20. The diluted samples were placed over conventional transmission electron microscopy (TEM) grids and allowed to set for 15 s. The background was stained with phosphotungstic acid solution 10.0% w/w (Sigma-Aldrich, St. Louis, MO, USA) for an additional 15 s.

2.6. Thermal analysis

BPQ crystallization behavior in NLC was carried out by using differential scanning calorimetry (DSC). Free BPQ, V1 and unloaded V1 were characterized in a DSC 4000 Perkin Elmer cell (Perkin Elmer Corp., Norwalk, CT, USA), under a dynamic N_2 atmosphere (50 mL.min^{-1}), using sealed aluminum capsules with about 2 mg of samples. DSC curves were obtained at heating rate of 10 °C.min^{-1} in the temperature range from 25 to 290 °C. An empty sealed pan was used as reference.

2.7. Saturation solubility evaluation

Free BPQ and BPQ-NLC solubility were evaluated in simulated gastric fluid (pH 1.2) and the following pharmacopoeial buffers: pH 4.5; 6.8; 7.4. Also, FaSSIF (Fasted State Simulated Intestinal Fluid) and FeSSIF (Fed State Simulated Intestinal Fluid) were prepared as described previously (Jogia et al., 2014), phosphate buffer 0.05 M (pH 7.4) with sodium dodecyl sulfate (SDS) (1.0% w/w); and phosphate buffer 0.05 M (pH 7.4) with Tween 80 (0.07% w/w) were evaluated.

The shake flask method was applied as follows: after shaking the BPQ saturated media for 24 h at 37 °C, the samples were filtered through PVDF 0.1 μm pore size membranes and diluted with the mobile phase at least 2-fold. The quantification of BPQ in the samples was performed with HPLC, as cited in Section 2.2.

2.8. Free BPQ and BPQ- NLC dissolution studies

The dissolution studies of free BPQ and BPQ-NLC were performed in a) phosphate buffer 0.05 M (pH 7.4) with Tween 80 0.07% w/w, with and without pancreatin (0.1% w/w); b) phosphate buffer 0.05 M (pH 7.4) with sodium dodecyl sulfate (SDS) 1.0% w/w, according to USP monograph for fenofibrate capsules test 2, found in the Dissolution Methods Database (United States Phamacopoeia, 2019). Pancreatin was added aiming to mimic the nanoparticle degradation from intestinal lipases released in the duodenum.

Dissolution settings were: medium volume of 900 mL, apparatus II (paddle), 50 rpm, sample volume of 2.0 mL, with media replacement for 60 or 90 min. The samples were filtered with a saturated membrane of PVDF 0.1 μm pore size and diluted with the mobile phase at least 3-fold. For each formulation and medium, the tests were performed in replicates of six. The BPQ quantification was performed by HPLC, as cited in Section 2.2.

2.9. Cytotoxicity and leishmanicidal activity

The optmized formulation V1 (402.5 ± 1.2 ug/mL of BPQ) described in the Section 3.1 was selected due to the highest surfactant concentration and smallest particle size. Cell viability was determined by the MTT method (3-methyl- [4–5-dimethylthiazol-2-yl] −2,5-diphenyltetrazolium bromide) as described by Monteiro et al., 2017 (L. M. Monteiro et al., 2017). For mammalian cells, mouse peritoneum macrophages were incubated for 24 h at 37 °C (2×10^5). Free BPQ was dissolved in DMSO (1% w/v) and BPQ-NLC V1 was diluted with RPMI to achieve concentrations in the range of 0.2 to 28 μM. Both preparations were added to the wells. After 24 h, MTT solution (5 mg.mL^{-1}) was added, and the plate was incubated at 37 °C, 5% CO_2, 95% RH, for 4 h. The optical density was measured in a microplate spectrophotometer (λ = 595 nm) (Multiskan™ GO Thermo Scientific™, Finland). Each treatment was evaluated with replicates of six. Cell-free and culture medium containing macrophages were used as a negative and positive control, respectively.

For amastigote test: L. *infantum* infected macrophages (1×10^6) were incubated (37 °C, 24 h) with increased concentrations of BPQ and BPQ-NLC V1. The cells were stained with giemsa and the number of infected, uninfected cells ($n = 200$) and amastigotes per cell were counted by microscopic examination.

The CC_{50} and IC_{50} values were calculated by non-linear regression analysis using GraphPad Prism version 5.01 (GraphPad Software, Inc., USA). All the experiments have been carried out under the approval of the Institute of Tropical Medicine of São Paulo ethics committee (registration number: CPE-IMT000269A June 5, 2014).

2.10. In vitro immunomodulatory effects of BPQ-NLC

The J774A.1 macrophage cell line was cultured in RPMI 1640 medium (Gibco) with 100,000 U/L penicillin and 100 mg/L streptomycin (Sigma), supplemented with 5% Fetal Bovine Serum (Gibco). Cells were grown in T25 culture flasks at 37 °C in a 5% CO_2 humidified incubator. Every 2 days, the cells were detached from the culture flask with a cell scraper and sub-cultured. The cells were counted and plated in 24-well plates (Corning) at 5×10^5 cells/well, and incubated overnight. After being washed with RPMI 1640 medium, the cells were treated with NLC or BPQ-NLC at 1, 5, or 10 μM, or stimulated with *Escherichia coli* O111: B4 Lipopolysaccharide (LPS; Sigma) at 1 μg/mL, or left in medium. After 6, 24, 48 and 72 h, the culture supernatants were harvested and analyzed to determine the cytokine levels. The concentrations of the released mediators IL-1β, IL-6, and TNF-α were determined by ELISA kits (Invitrogen) in accordance with the manufacturer's protocols.

For the comparisons between the effects of different concentrations of NLC and BPQ-NLC (V1) on the levels of cytokines, the one-way ANOVA test was used, with Bonferroni's post hoc test, and for the comparisons between the incubation periods of 6, 24, 48 and 72 h, the Repeated Measures ANOVA test was used, also with Bonferroni's post hoc test. The analyses were conducted on the GraphPad Prism software (GraphPad Software). Results were presented as mean with SEM, and p values ≤ 0.05 ($\alpha = 0.05$) were considered statistically significant.

2.11. In vivo leishmanicidal activity and DNA quantification by real-time PCR

Gold Syrian hamsters (*Mesocricetus auratus*) is considered the most suitable model to evaluate visceral leishmaniasis disease. It has the closest immunologic features compared to human visceral leishmaniasis among all available animals (Jiménez-Antón et al., 2019; Melo et al., 2017; Melby et al., 2001). L. *infantum* (MHOM/BR/1972/LD) was investigated since it is the most relevant and responsible for VL in human and dogs in the New World, especially in Brazil (Michel et al., 2011). For the *in vivo* evaluation, BPQ-NLC V1 (402.5 ± 1.2 ug/mL of BPQ) was selected due to the smallest particle size.

Young male Golden hamsters (<110 g) were infected intraperitoneally with L. *(L.) infantum* promastigotes (1 × 108/animal). Forty days after the infection, the hamsters ($n = 5$/group) were treated in fasted condition by oral route for 10 consecutive days as follows: BPQ-NLC at 0.3 mg/kg/day (0.9 mol/kg/day), which corresponds to 0.12 mL per animal, miltefosine at 2.0 mg/kg/day (4.9 mol/kg/day) and blank-NLC.

Control group was untreated animals. The animals were euthanized 50 days post-infection. The BPQ doses were based in the previous study by Reimão and colleagues (2012) (Reimão et al., 2012). The miltefosine dose were based in the therapeutic recommendation for dogs.

The spleen and liver were removed, weighed, and the number of DNA copies per mg of tissue was quantified by real-time polymerase chain reaction (RT-PCR). DNA purification was performed using Qiagen DNeasy Blood and Tissue Kit (Qiagen, Germany). Around 20 mg tissue from the liver and 10 mg of spleen were placed into a clean 1.5 mL microcentrifuge tube, then followed manufacturer instructions. The quantity and quality of DNA were determined using NanoDrop Lite Spectrophotometer (Thermo Scientific, USA). Tissues of non-infected animals were used as controls.

Leishmania HPS70 heat protein shock sequence (234 bp. HSP70F: GGA CGAGATCGAGCGCATGGT. HSP70R: TCCTTCGACGCC TCCTGGTTG) was used for quantification. Sybr Green real-time PCR was set up with Maxima SYBR Green/ROX qPCR Master Mix (2X), 100 nM final concentration of forward and reverse primers, 5 µL of DNA of the sample, control (tissue of non-infected animal) or cloned DNA (quantification curve from10^{-1} to 10^{6} DNA copies), in a total volume of 20 µL. Amplification was performed in a real-time instrument (StepOne Real-Time PCR System, Thermo Fisher/Applied Biosystems) with the following conditions: polymerase activation at 95 °C for 5 min, followed by 40 cycles of 94 °C for 25 s, 60 °C for 20 s, and 72 °C for 30 s. Followed by a holding stage of 72 °C for 2 min. The melting curves (for the amplification specificity) were determined at 70 °C (45 s) and an increase in the temperature to 95 °C.

Statistical analysis was performed by ANOVA ($\alpha = 0.05$) and Dunnett's Post Hoc Test, using Minitab 19. All the experiments have been carried out under the approval of the Institute of Tropical Medicine of São Paulo ethics committee (registration number: 000417A, November 25th, 2019).

3. Results and discussion

3.1. Development of BPQ-NLC

Previous screening experiments showed only one critical process parameter. When the number of cycles is three or less, the drug could not be accommodated in the lipid structure, and precipitation occurred. Therefore, all preparations were performed using five cycles of homogenization. Table 2 shows the design matrix and the experimental results of Z-average, PDI and zeta potential for each preparation. The influence of the factors (SL:L,% poloxamer 188,% lipid phase) and their interactions in the Z-average are shown in the contour plots (Fig. 1).

The lipid phase and poloxamer 188 have a nonlinear relationship, and BPQ-NLCs with Z-average lower than 220 nm can be achieved with a combination of lipid phase lower than 10.0% w/w and poloxamer 188 higher than 3.5% w/w (Fig. 1C). The negligible impact of SL:LL in the Z-average is observed when the% lipid phase is lower than 7.5% w/w (Fig. 1B). The ratio can be changed from 0.5 to 3, but the Z-average only varies from 200 to 225 nm. The absence of the <200 nm zone (Fig. 1C) indicates that nanoparticles in this range are only possible to prepare when poloxamer 188 is above 2.5%.

The variables% lipid phase ($p < 0.05$; $\alpha = 0.05$) and% poloxamer 188 ($p < 0.05$; $\alpha = 0.05$) showed significant effect on the output (Z-average). SL:LL has a low impact in the Z-average, as revealed by the non-significant p value (>0.05) (suplementary data). The goodness-of-fit indexes, the lack-of-fit (p value >0.05; $\alpha = 0.05$), and R^2 of 96.37% and adjusted-R^2 (93.95%) corroborate the suitability of the model, which means that the factors explain most of the variability. The mathematical model to predict Z-average is described in Eq. (3):

$$Z - \text{ave} = 173.8 + 9.0\ \text{SL} : \text{LL} - 5.6\ \%\text{POL} + 15.7\ \%\text{LP} - 3.2\%\text{POL x }\%\ \text{LP} \quad (3)$$

Where Z-ave: Z-average (nm);% POL:% w/w of Poloxamer 188;% LP:% w/w of lipid phase.

For the mathematical model verification two preparations were obtained: V1 (predicted Z-average: 175.3 nm, SL:LL 1.0, 4.0% w/w poloxamer 188, and 5.0% w/w lipid phase) and V2 (predicted Z-average: 253.3 nm, SL:LL 0.5, poloxamer 188 3.0% w/w and lipid phase 15.0% w/w). The predicted and observed Z-average values for both formulations were in the range of the model (95% CI), confirming the equation suitability. They showed zeta potential of −17.3 mV for V1 and −29.2 mV for V2, low PDI (<0.3) and monomodal particle distribution. Hence, V1 and V2 were further evaluated.

The poloxamer 188 concentration showed an inverse relation effect in the Z-average; the lowest Z-averages were achieved using the highest concentration of the surfactant. This performance can be explained by the reduction in the interfacial tension between the dispersed and continuous phases. With the increase in the content, more surfactant is available for adsorption in the newly developed surface of the particles, during the homogenization process (Witayaudom and Klinkesorn, 2017). The opposite performance was found in the% lipid phase, which can be supported by the same mechanism. With an increase in the amount of the lipid phase, more surfactant is required for packing on the particle surface (Sznitowska et al., 2017). Another possible mechanism was previously described: the increase in the particle size due to the increment in the amount of lipids can be explained by the reduction in dispersion energy available per unit of lipid, using the high-energy method (Savić et al., 2019).

The structure of NLC depends on the amount of liquid lipid, being the main factor for reducing the crystallinity of the lipid matrix. The SL:LL factor showed that the increase in the amount of LL does not affect the Z-average in the range of 0.5 to 3, the lowest and highest levels, respectively (Table 1). Therefore, the lower ratio was applied in V1 and V2 preparations, aiming to increase the drug loading and to reduce the possibility of crystallinity changes during the storage. A similar result was described in the preparation of NLC with different ratios of Precirol,

Table 2
Experimental design matrix, Z-average (Z-ave), polydispersity index (PDI) and zeta potential (ZP) of BPQ-NLC.

SO	Level SL:LL	% POL	% LP	SL:LL	% POL	% LP	Z-ave (nm)	PDI	ZP (mV)
F11	0	0	0	1.75	2.5	10.0	231.8	0.164	−22.1
F9	0	0	0	1.75	2.5	10.0	235.5	0.155	−12.8
F8	+1	+1	+1	3.00	4.0	15.0	229.3	0.147	−15.3
F1	−1	−1	−1	0.50	1.0	5.0	239.9	0.158	−20.4
F5	−1	−1	+1	0.50	1.0	15.0	366.9	0.241	−30.6
F4	+1	+1	−1	3.00	4.0	5.0	198.1	0.192	−19.3
F7	−1	+1	+1	0.50	4.0	15.0	208.3	0.164	−24.0
F6	+1	−1	+1	3.00	1.0	15.0	390.6	0.250	−43.7
F10	0	0	0	1.75	2.5	10.0	232.6	0.143	−27.0
F2	+1	−1	−1	3.00	1.0	5.0	267.7	0.223	−28.2
F3	−1	+1	−1	0.50	4.0	5.0	180.6	0.180	−25.3

SO: standard order; SL:LL: solid lipid to liquid lipid ratio;% POL: percentage of poloxamer 188 (w/w);% LP: percentage of lipid phase (w/w).

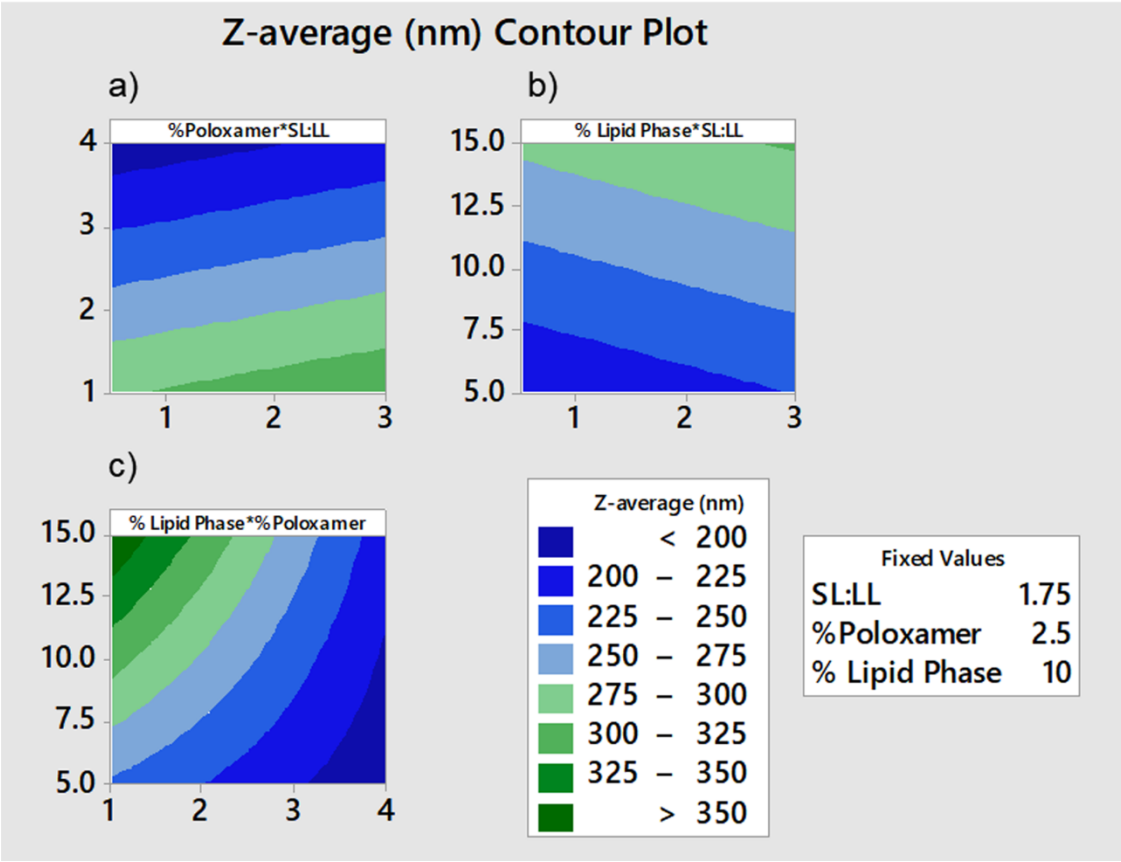

Fig. 1. Contour plot of Z-average from buparvaquone nanostructured lipid carrier development using the design space approach.

as a solid lipid, and Capryol 90, as a liquid lipid (Date et al., 2011). They showed that an increase of liquid lipid up to 50% of the total lipid phase did not change the particle size or PDI of the preparations. Besides, in the development of NLC prepared with cetyl palmitate and Miglyol 812, the Z-average was not significantly affected, with an increase of Miglyol 812 also up to 50% (Teeranachaideekul et al., 2008). It was claimed that the viscosity of the lipid phase, in the homogenization process temperature (approximately 80 °C), of different oils content, should be similar, and the shear rate should have the same effect in the lipid phase breaking down. The non-linear relationship between% lipid phase and% poloxamer is described in the mathematical model (−3.2% POL ×% LP). The negative coefficient suggests a synergistic interaction in the reduction of the Z-average. The possible mechanism is the effect of poloxamer P188 on lipids. Their interaction forms a tight and high orderly structure (Wu et al., 2004; Adhikari et al., 2016).

The components used for BPQ-NLC development are commercially available and applied in pharmaceutical products (Beloqui et al., 2016). This drug delivery system has the potential to provide affordable medicines due to the low cost of raw materials, comparing with the phospholipids used in liposomes. However, NLCs remain an expensive formulation due to the cold-transport chain which significantly impacts on cost of therapy, similarly to COVID-19 vaccines. This is especially relevant considering that the leishmania has strong and complex links with poverty. Hence, it is mandatory a public policy to assure the treatment to this vulnerable population.

Besides high-pressure homogenization technology is well-established, reproducible, and shows scale-up feasibility (L.M. Monteiro et al., 2017). Although leishmaniasis is prevalent in tropical countries, the stability was not considered a limiting factor since the formulations showed stability at 4 °C (supplementary material). In addition, other leishmaniasis medicines are commercialized in lower temperatures, *i.e.*, liposomal amphotericin B."

3.2. Morphology by transmission electron microscopy (TEM)

The morphology of V1 and V2 formulations by transmission electron microscopy are shown in Fig. 2. The photon correlation spectroscopy (PCS) technique is an indirect method for nanoparticle size evaluation. Therefore, a complementary method must be applied to confirm size and morphology. The diffusion coefficient (D) is used in the Stokes-Einstein equation for the hydrodynamic size calculation. Anisotropic particles have different D value than round ones. As a result, particles with the same size, but distinct morphologies will not have the same results in PCS analysis (Stetefeld et al., 2016). Fig. 2 shows the round shape of V1 (173.9 ± 1.6 nm) and V2 (232.4 ± 1.6 nm) in the nanometric range. Thus, Z-average results from V1 and V2 can be considered reliable.

3.3. Thermal analysis

The thermal behavior of BPQ, NLC and BPQ-NLC are presented in Fig. 3. DSC curve of BPQ showed one sharp endothermic event in the temperature range 170 to 180 °C (T_{onset} = 177 °C; T_{peak} = 183 °C), assigned to the melting process (L.M. Monteiro et al., 2017). For BPQ-NLC and NLC, endothermic events were observed at onset temperatures of 40 and 43 °C, whereas for the exothermic events the onset temperatures were 153 and 177 °C, respectively.

DSC analysis was performed to select solid lipids to prepare BPQ-NLC (L.M. Monteiro et al., 2017). The assessment was based on the capacity of the melted lipid to solubilize the drug in heating cycles experiments. Softisan® 154 had the best ability to solubilize the drug. Herein, the DSC curves of BPQ-NLC and NCL showed an endothermic event that corresponds to Softisan® 154 melting in the range of 53–58 °C (L.M. Monteiro et al., 2017). It is followed by an exothermic event at 177 °C, which might indicate thermal degradation of lipids (Softisan® 154 and MCT). However, the complete absence of the BPQ melting peak in the DSC

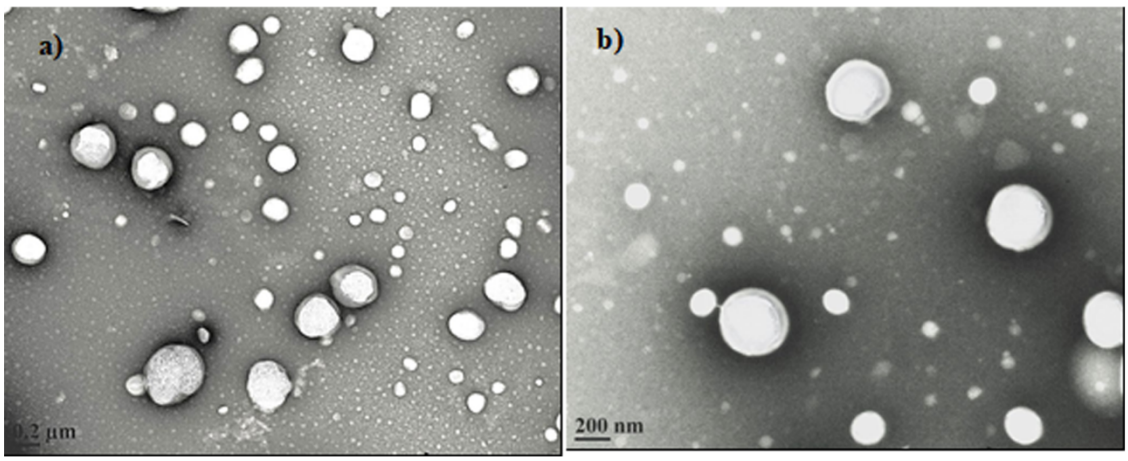

Fig. 2. Transmission electronic microscopy of formulation: a) V1; b) V2. Magnification 36kx.

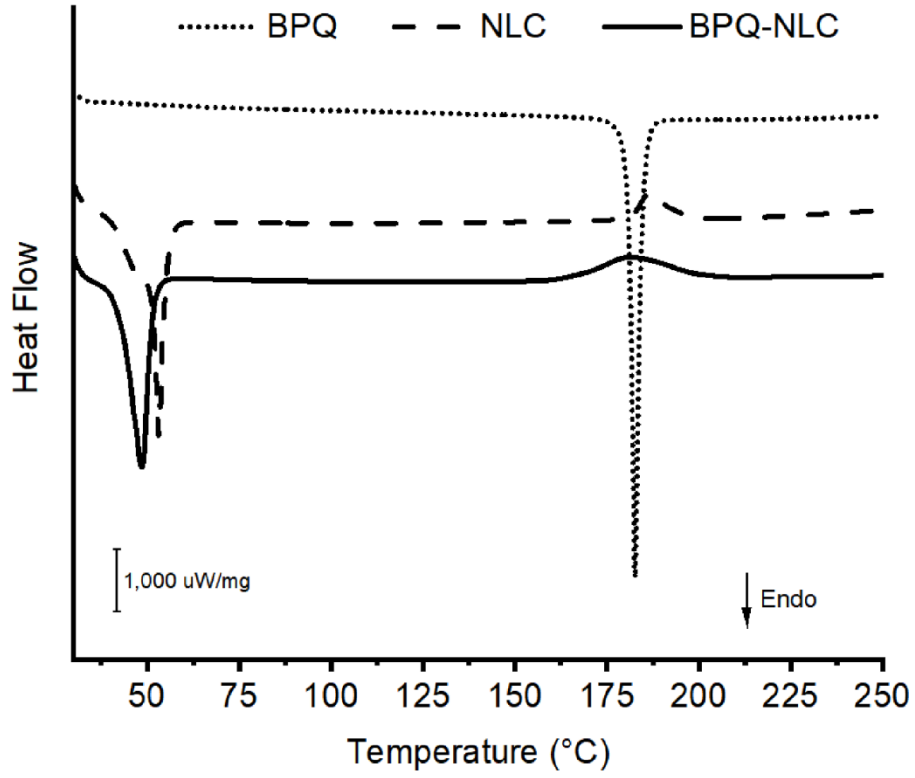

Fig. 3. DSC curves of free burpavaquone (PQB), unloaded nanostructured lipid-carrier (NLC) and V1 formulation (BPQ-NLC) obtained under a dynamic N_2 atmosphere (50 mL.min^{-1}) at heating rate of 10 °C.min^{-1}.

profile of BPQ-NL indicates that the drug molecule was solubilized in the lipidic matrix, which is congruent with its high lipophilicity (Reimão et al., 2012) and the high entrapment efficiency (~99%) here obtained (supplementary data). Further, both Softisan® 154 melting peak and posterior lipid degradation event are depressed for BPQ-NLC, when compared to the unloaded carrier, which reinforces the good miscibility of BPQ in the lipidic matrix (Zoubari et al., 2017).

3.4. Saturation solubility evaluation

The solubility of free BPQ and BPQ released from NLC preparations V1 and V2 are shown in Table 3. Free BPQ showed limited solubility, except in the Fed State Simulated Intestinal Fluid and phosphate buffer pH 7.4 with sodium dodecyl sulfate 1.0% w/w, which revealed the surfactant dependence for BPQ solubilization. Both V1 and V2 showed improved BPQ saturation solubility.

BPQ-NLC V1 showed an increase in solubility from 2.0 (FeSSIF) to 73.0-fold (pH 1.2) compared to the free drug. For V2 the increase was from 1.5 (pH 7.4 + SDS 1.0% w/w) to 72.8-fold (pH 1.2). The oral administration of BPQ-NLC can be feasible despite the low solubility in the media without surfactant (Table 3) since bile salts and lipases are released in the mammalian gastrointestinal fluid from the duodenum. These bio-surfactants and enzymes could promote BPQ release from the lipid matrix reducing the drug precipitation; as a result, improving its absorption. Thus, this test allowed selecting the media for the BPQ-NLC dissolution profile study, and it corroborated the potential use of NLCs for improving poor-water soluble drugs.

Table 3
Saturation solubility of free BPQ and V1 and V2 preparations of BPQ-NLC ($n = 3$).

Media	Saturation solubility (μg.mL^{-1})		
	Free BPQ	V1	V2
SGF pH 1.2	0.05 ± 0.01	3.57 ± 1.72	3.64 ± 2.20
PB pH 4.5	0.06 ± 0.04	3.30 ± 0.98	2.78 ± 0.90
PB pH 6.8	0.08 ± 0.02	2.82 ± 1.41	2.77 ± 3.05
PB pH 7.4	0.19 ± 0.10	12.62 ± 1.52	2.16 ± 0.65
FeSSIF pH 5.0	12.53 ± 1.85	24.98 ± 2.04	25.56 ± 1.12
FaSSIF pH 6.5	3.39 ± 0.24	26.30 ± 2.66	2.28 ± 0.85
PB pH 7.4 + SDS 1.0% w/w	11.68 ± 0.78	37.74 ± 10.66	17.08 ± 4.50
PB pH 7.4 + T80 0.07% w/w	3.39 ± 0.30	15.31 ± 7.05	9.19 ± 2.02

SGF: simulated gastric fluid; PB: phosphate buffer; FeSSIF: fed state simulated intestinal fluid; (FaSSIF): Fasted state simulated intestinal fluid; SDS: sodium dodecyl sulfate; T80: Tween 80.

3.5. Free BPQ and BPQ- NLC dissolution studies

The dissolution profiles of V1 and V2 formulations in phosphate buffer pH 7.4, 0.05 M with Tween 80 (0.07% w/w) with or without pancreatin (0.1% w/w), and in phosphate buffer pH 7.4, 0.05 M with sodium dodecyl sulfate (1.0% w/w) are shown in Fig. 4.

Dissolution profiles of free BPQ and BPQ-NLC were first tested in simulated gastric fluid pH 1.2, phosphate buffer pH 4.5, and pH 6.8. However, no BPQ was dissolved during 24 h of testing, which shows the potential development of a delayed dosage form. The requirement of a surfactant for drug release was observed, as found in the saturation solubility test. Through oral administration, these BPQ-NLC would avoid drug release and precipitation in the stomach since gastric lipolysis is limited due to low enzyme content and its pH activity profile (Minekus et al., 2014; Torcello-Gómez and Foster, 2014).

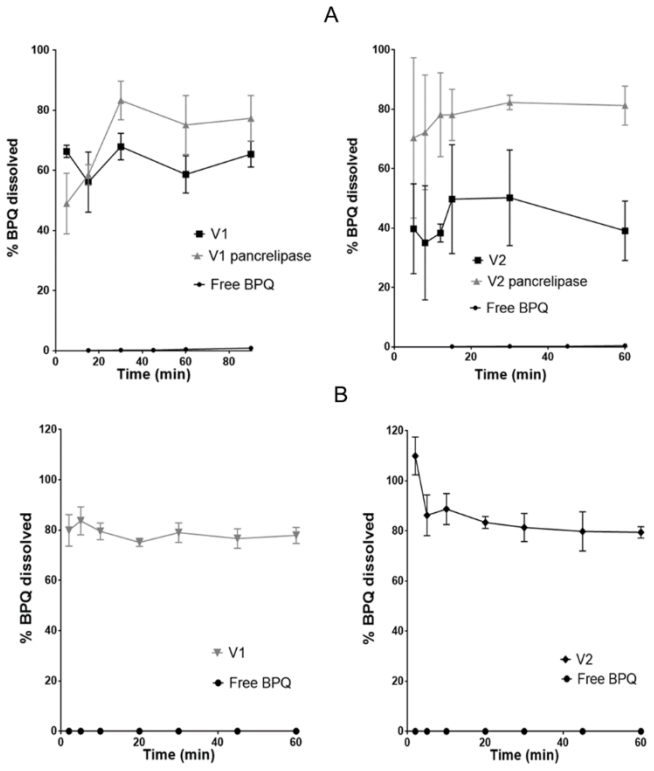

Fig. 4. BPQ dissolution of free BPQ (4 mg) (black circles) and BPQ-NLC formulations (containing 4 mg) using USP II apparatus, at 50 rpm, in 900 mL phosphate buffer pH 7.4, 0.05 M with: A) Tween 80 (0.07% w/w) with (gray triangles) and without (black squares) pancrelipase, or B) sodium dodecyl sulfate 1.0% w/w. V1 [Z-average: 173.9 ± 1.6 nm]; V2 [Z-average: 232.4 ± 1.6 nm].

Free BPQ dissolution in phosphate buffer pH 7.4, 0.05 M with Tween 80 was limited (Fig. 4A). After 60 min, 0.43% of the 4.0 mg of the free drug was dissolved. Even after four hours, only 2.89% was dissolved. In the dissolution profiles with SDS (Fig. 4B), the free drug could not be dissolved despite the increased surfactant content. At the end of 60 min, the% dissolved was below the detection limit of the HPLC method. The interaction with the anionic surfactant can explain the poor drug dissolution. The BPQ ionization was simulated by the software Chemicalize™ (ChemAxon, Hungary). Above pH 6.0, the drug is dissociated with an anionic charge; it was supposed to dissolve due to a reduction in the interfacial tension, but precipitation occurred when BPQ ions interacted with the charges of SDS. The solubility of the compound PG-300,995 in different pH and concentrations of SDS was also assessed. The drug precipitated in pH >7.0 where both molecules are ionized due to an insoluble salt formation (Jain et al., 2004).

In contrast, the dissolution profile of V1 in phosphate buffer pH 7.4 with Tween 80 without pancreatin could reach 58.66% of the 4.0 mg drug dose after 60 min (Fig. 4A). With the addition of the enzyme, 75.15% of BPQ was dissolved. However, it is important to note that in this condition, it was observed drug precipitation. After 30 min, the dissolution with and without pancreatin was 83.29% and 67.93%, respectively. In contrast, SNEDDS dissolution profile in the simulated gastric fluid showed a burst in the first 10 min and reached a plateau up to 50 min. A complete release of BPQ was observed within 30 min after the pH was increased to 6.8. The authors emphasized that avoiding precipitation may improve BPQ oral absorption (Smith et al., 2018).

V2 showed a release comparable to V1 in media containing Tween 80 with the enzyme, but slower release in medium without pancrelipase (Fig. 4A). From V2, after 60 min, 81.25% and 39.07% of 4.0 mg dose were dissolved, with and without enzyme, respectively. The higher V2 Z-average can explain the release in the medium without pancreatin compared with V1 (Fig. 4A). With the reduction in the particle size, the surface area is increased; thus, improved BPQ solubility and dissolution are expected (Üstündağ-Okur et al., 2016).

Targeting the intestines, the drug must be dissolved only when it enters the duodenum, where bile salts and pancreatic fluids are released in response to lipid ingestion. These fluids contain multiple lipases, such as pancreatic lipase, pancreatic lipase-related protein 2, carboxyl ester lipase and phospholipase A2 (Lowe and Whitcomb, 2015). Hence, we hypothesized that this physiological mechanism may allow the BPQ release from NLC throughout GIT (pH >6.4).

BPQ dissolution from both NLCs preparations in medium with SDS was increased. V1 and V2 avoided the drug precipitation, as compared with free BPQ, despite the precipitation by the interaction with SDS charges. The delayed BPQ release showed the potential for BPQ intestine delivery. A similar performance *in vitro* dissolution of NLC containing vitamin D3 was found (Park et al., 2017). In gastric conditions, less than 4.0% of the vitamin was released after seven hours of testing. Still, the release in the simulated intestinal fluid was 90% after eight hours due to lipase activity.

3.6. Cytotoxicity and leishmanicidal activity

The cytotoxicity against mammalian cells of free BPQ and BPQ-NLC, resulted in a CC_{50} of 554.4 μM (95% CI: 252.2–1090.0) and of 583.4 μM (95% CI: 362.6–938.6) for free BPQ and V1, respectively. The IC_{50} against L.*infantum* amastigotes from free BPQ was 456.5 nM (95% CI: 332.4 - 627.0). From BPQ-NLC, the IC_{50} was 229.0 nM (95% CI: 190.5 - 275.2). Selective index of free BPQ and BPQ-NLC were 1149 and 2548, respectively.

Reimão et al. (2012) (Reimão et al., 2012) found BPQ IC50 using L. *infantum chagasi* amastigotes of 1.50 μM (1.41–1.62) or 1500 nM, while Croft and colleagues (1992) (Croft et al., 1992) found IC50 of 50 nM for L. *donovani* amastigotes. Therefore, we considered that these discrepancies (50, 456.5 and 1500 nM) may be explained by the methodology difference and parasite sensitivity. Thus, we consider that due this

variability direct comparison with literature were not possible. However, Reimão and colleagues (2012) (Reimão et al., 2012) and Thapa and colleagues (2021) (Thapa et al., 2021) showed the safety and high selective index (>10) of free BPQ. The present results corroborated the previous studies and showed increased selective index of BPQ in nanostrucutured systems as found by Thapa and colleagues (2021). Their study also showed an increase of 13-fold in the selective index of nanostructured BPQ against amastigotes of L. donovani when compared to free BPQ.

3.7. *In vitro immunomodulatory effects of BPQ-NLC*

The *in vitro* immunomodulatory effects of BPQ-NLC were assessed by evaluating the cytokines levels in cultures of J774A.1 cells treated with different concentrations of NLC or BPQ-NLC (V1). As expected, the positive control of LPS stimulation resulted on high levels of IL-1β, IL-6, and TNF-α (data not shown). There were no detectable levels of IL-1β and IL-6 with the treatment with either BPQ-NLC or NLC. On the other hand, TNF-α was detected on cultures of cells treated with 1 or 5 μM of BPQ-NLC or NLC, and at similar levels to those observed on cells in Medium alone (Fig. 5). The 10 μM dosage of both formulations induced a significant decrease of TNF-α, especially after 6 and 24 h of incubation.

The absence of higher TNF-α level on NLC or BPQ-NLC treated cells compared with cells in Medium showed that these formulations do not stimulate an unspecific immune response. Similar results were observed with the nanoliposomal buparvaquone treatment of murine peritoneal macrophages (Costa-Silva et al., 2017). Furthermore, the highest dosage of both NLC and BPQ-NLC decreased the secretion of this cytokine, which is particularly important during visceral leishmaniasis. The overexpression of TNF-α was associated with higher proliferation of parasites and chronic infection (Murray, 2001). The lack of IL-1β and IL-6 production after treatment with NLC or BPQ-NLC in the present study may also be beneficial. *Leishmania* spp. are known to induce the production of these cytokines in the host cells with protective effects, along with TNF-α. On the other hand, disease severity is associated with an uncontrolled inflammation caused by excessive amounts of IL-1β, IL-6, and TNF-α (Meira and Gedamu, 2019).

3.8. *In vivo leishmanicidal activity*

For decades, viceral leishmaniasis has been treated with injectable pentavalent antimonials, and only miltefosine has been approved for administration by oral route (Sunyoto et al., 2018). Nevertheless, this drug substance never became affordable and available for patients who most need the treatment (Sunyoto et al., 2018). Besides, the development of resistance has increasing concerns about the effectiveness of miltefosine drug therapy (Reimão et al., 2020). Hence, the aim of this work was to evaluate whether BPQ-NLC presents *in vivo* activity against L. *infantum*.

Fig. 6 shows the leishmanicidal activity of BPQ-NLC V1 (0.3 mg/kg/day) and miltefosine (2.0 mg/kg/day), in the spleen and liver. V1 parasite burden reduction in spleen was 94.4% ± 6.0% ($p > 0.05$; $\alpha = 0.05$), while in the liver 83.4% ± 18,2% ($p < 0.05$; $\alpha = 0.05$). For miltefosine it was 92.8% ± 7.9% and 87.2% ± 14.2% in the spleen and in the liver, respectively. For both treatments the parasite burden was reduced when compared to the control (untreated group). In addition, the statistical analysis showed that there is no difference between blank-NLC and control group, for both spleen and liver. The ANOVA p value for the liver and the spleen were <0.05 ($\alpha = 0.05$) and >0.05, respectively. The statistical significance for the spleen could not be achieved due to the high variability of the control. Despite the non-statistical significance for the spleen results, the box plot shows the difference between control and the BPQ-NLC treated group.

A liposome formulation containing BPQ was tested in L. *infantum*-infected hamsters (Costa-Silva et al., 2017). Initially, three routes of administration were evaluated: sub-cutaneous, intramuscular and intravenous, at 0.4 mg/kg/day (1.2 mol/kg/day), for 10 consecutive days. Sub-cutaneous treatment showed the best efficacy, reducing the parasite burden in the spleen and liver by 98 and 96%, respectively. For authors, the effectiveness of the formulation could be due to a depot effect, which could sustain BPQ release from possible intact nanoparticles. Besides, they also discussed the possibility of drugs reaching the lymphatic system when using injectable liposomes. In this case, the drug could enter the lymphatics by reaching lymph nodes in the site of the lesion, which is a gateway to pathogen dissemination (Costa-Silva et al., 2017; Thomaidou et al., 2015).

Herein, the expected drug release mechanism involves the digestion of the lipids and the presence of bio-surfactants, both contributing to BPQ solubilization and absorption. The lymphatic system is also associated with oral lipid formulations, but in this case the hypothesis is based on drugs entering the lymphatics by chylomicron pathway. It states that after digestion of lipid formulations, drug and lipids could be packing in the enterocytes during chylomicron synthesis (Vishwakarma et al., 2019). In the case of BPQ, its high lipophilicity justifies the

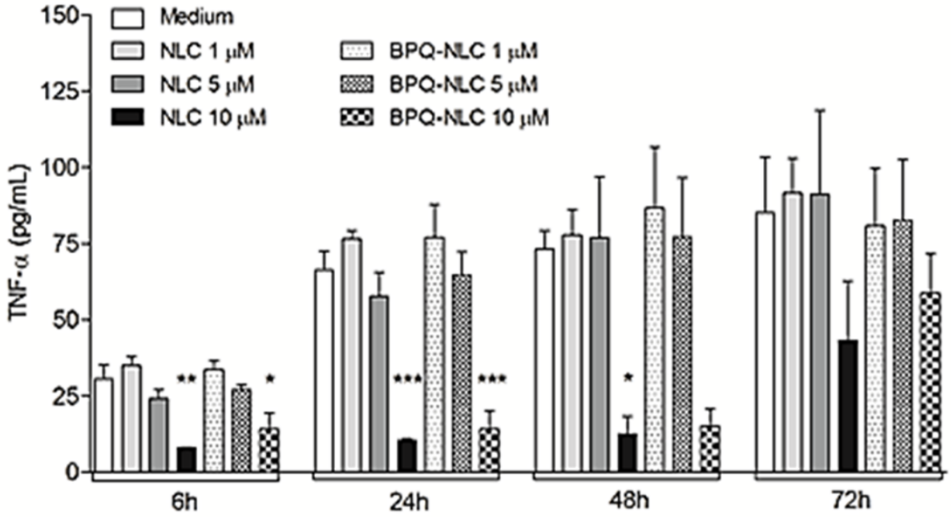

Fig. 5. Levels of TNF-α after treatment with NLC or BPQ-NLC. The levels of TNF-α were determined by ELISA assay on supernatants from cultures of J774A.1 macrophages treated with NLC or BPQ-NLC at 1, 5, or 10 μM after 6, 24, 48 and 72 h of incubation. Results presented as means with SEM; *$p \leq 0.05$; **$p \leq 0.01$; and ***$p \leq 0.001$ compared with Medium at the respective period of incubation.

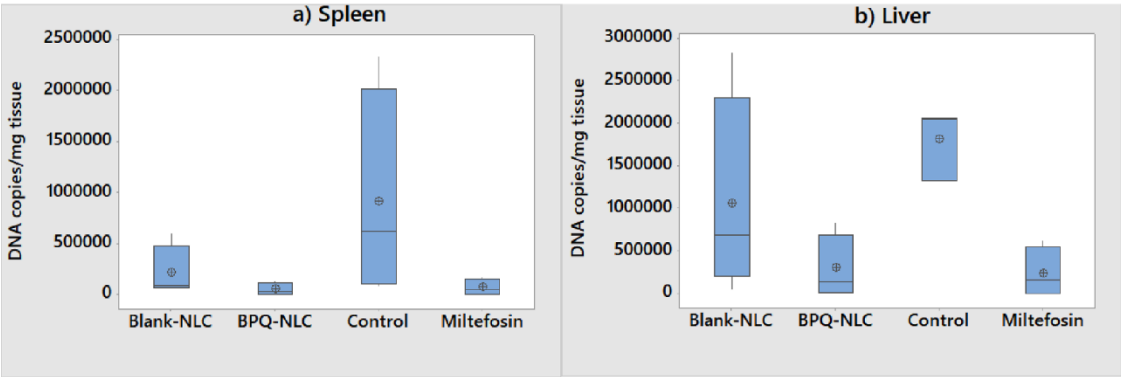

Fig. 6. Leishmanicidal activity after oral administration (10 consecutive days) of BPQ-NLC (0.3 mg/kg/day), Miltefosine (2.0 mg/kg/day), blank-NLC and control (untreated group) in a) spleen and b) liver (n = 5/group, young male Golden hamsters <110 g).

possibility, but other factors such as particle size or chain length of triglycerides may impact the phenomenon (Vishwakarma et al., 2019).

A BPQ self-nanoemulsifying drug delivery system (SNEDDS) was tested in L. *infantum*-infected BALB/c mice (Smith et al., 2018). The BPQ dose was 6.0 mg/kg/day, once daily for 10 consecutive days. The parasite burden reduction in spleen was 94%, and in the liver it showed values of 48 and 56%. Authors attributed the lower activity in the liver to a possible BPQ metabolism by CYP enzymes (2C9, C19 and 3A4) from mouse liver microsomes. They proposed developing SNEDDS with CYP inhibitor fluconazole, besides reducing the amount of long-chain and increasing the amount of short and medium-chain tryglycerides in the formulation, which could diminish liver accumulation of the product to improve BPQ effect.

In our study BPQ parasite reduction in the liver was 83% and close to reference drug miltefosine (87%). Preclinical studies showed that miltefosine is slowly and almost completely absorbed in rats and dogs (Dorlo et al., 2012). Considering its slow elimination and high accumulation (Dorlo et al., 2008), no issues related to bioavailability seems to be associated with this drug substance. The lower parasite reduction of both compounds in the liver might be hyphotesized to an early leishmania proliferation in this organ; the spleen, in turn, might serve as a resevoir (Meira and Gedamu, 2019). Hence, a higher dose could provide a better efficacy result in the liver, but this approach should be accompanied with safety monitoring in clinical studies.

The dose of miltefosine was chosen for two purposes. First, to verify the validity of the animal model; second to estimate an initial dose of BPQ-NLC in one of the species of interest (dogs with visceral leishmaniasis). Therefore, the miltefosine dose was chosen considering that the leishmanicidal activity was statistically equivalent to the BPQ-NLC tested dose. Even being 3 times higher than the recommended dose, using body area equivalence as described by the FDA, there was no total elimination of parasites, as reported by Fortin et al. (2012) (Fortin et al., 2012), and by Hendrickx et al. (2015), which stated that even using 40 mg/kg dose, hamsters failed to eliminate L. *infantum* parasites with a 5-day treatment (Hendrickx et al., 2015). Therefore, the dose of 10 mg/kg provided a direct comparison of leishmanicidal activity in a possible future test of BPQ-NLC in dogs. Additionally, it turned out to be a suitable leishmanicidal activity amount to validate the animal model.

In this study, we aimed to develop BPQ-NLC for leishmaniasis oral treatment. Since the product showed equivalent efficacy as reference drug miltefosine, the possibility of combining the two drugs in a therapeutic regimen in the future could be considered. Multidrug therapy may provide therapeutic benefits such as lower doses, higher efficacy and better patient compliance. In addition, reducing dose may help to avoid the selection of drug-resistant lines of the parasite (Reimão et al., 2020). This is especially interesting considering the raising concerns about miltefosine monotherapy, which encourages the search for therapeutic regimens with better efficacy and safety outcomes (Reimão et al., 2020).

4. Conclusion

In this study we tested the hypothesis whether BPQ-NLC shows *in vivo* activity against L. *infantum* by oral administration. BPQ-NLC showed similar leishmanicidal activity compared to miltefosine, presenting parasite burden reduction higher than 80% in the liver. Therefore, our results supported that this formulation can enable safe and feasible oral therapy for the treatment of leishmaniasis. Thus, this study revealed a promising strategy for treating leishmaniasis, which can expand the limited therapeutic arsenal available for this disease. HPH successfully allowed the BPQ-NLC preparation with suitable particle distribution. Using a statistical approach, it was possible to understand the critical input variables,% lipid phase, and surfactant concentration and their interactions, which influenced the Z-average. The mathematical model derived from the study yield two optimized formulations, V1 (173.9 ± 1.6 nm) and V2 (232.4 ± 1.6 nm), both presented Z-averages close to predicted values, confirming the suitability of the model. BPQ solubility was improved significantly, reaching up 73.0-fold compared with free drug. The dissolution test showed the potential oral administration of the BPQ-NLC by the performance of bio-surfactants and lipolytic enzymes. The assessment of the stability testing data revealed the feasible development of a liquid dosage form, which was prepared using affordable lipids and direct scalable technology.

CRediT authorship contribution statement

Lis Marie Monteiro: Conceptualization, Investigation, Validation, Formal analysis, Writing – original draft. **Raimar Löbenberg:** Supervision, Methodology. **Eduardo José Barbosa:** Writing – review & editing. **Gabriel Lima Barros de Araujo:** Methodology. **Paula Keiko Sato:** Investigation, Formal analysis, Writing – review & editing. **Edite Kanashiro:** Investigation. **Raissa H. de Araujo Eliodoro:** Investigation. **Mussya Rocha:** Investigation. **Vera Lúcia Teixeira de Freitas:** Methodology. **Nikoletta Fotaki:** Writing – review & editing. **Nádia Araci Bou-Chacra:** Project administration, Funding acquisition, Resources, Writing – review & editing.

Declaration of Competing Interest

The authors declare that they have no known competing financial interests or personal relationships that could have appeared to influence the work reported in this paper.

Acknowledgments

This study was supported by the São Paulo Research Support Foundation (FAPESP) grant 2018/16028-5. This study was financed in part by the Coordenação de Aperfeiçoamento de Pessoal de Nível Superior – Brazil (CAPES) - Finance Code 001. The paper was revised by Jim Hesson (http://academicenglishsolutions.com/AES/home.html).

Supplementary materials

Supplementary material associated with this article can be found, in the online version, at doi:10.1016/j.ejps.2021.106097.

References

Adhikari, U., Goliaei, A., Tsereteli, L., Berkowitz, M.L., 2016. Properties of poloxamer molecules and poloxamer micelles dissolved in water and next to lipid bilayers: results from computer simulations. J. Phys. Chem. B 120, 5823–5830. https://doi.org/10.1021/acs.jpcb.5b11448.

Alavi, M., Hamidi, M., 2019. Passive and active targeting in cancer therapy by liposomes and lipid nanoparticles. Drug Metab. Pers. Ther. 34. https://doi.org/10.1515/dmpt-2018-0032.

Beloqui, A., Solinís, M.A., Rodrígues-Gascón, A., Almeida, A.J., Préat, V., 2016. Nanostructured lipid carriers: promising drug delivery systems for future clinics. Nanomedicine 12, 143–161. https://doi.org/10.1016/j.nano.2015.09.004.

Burza, S., Croft, S.L., Boelaert, M., 2018. Leishmaniasis. Lancet. 392, 951–970. https://doi.org/10.1016/S0140-6736(18)31204-2.

Costa Lima, S., Rodrigues, V., Garrido, J., Borges, F., Kong Thoo Lin, P., Cordeiro da Silva, A., 2012. *In vitro* evaluation of bisnaphthalimidopropyl derivatives loaded into pegylated nanoparticles against Leishmania infantum protozoa. Int. J. Antimicrob. Agents 39, 424–430. https://doi.org/10.1016/j.ijantimicag.2012.01.003.

Costa-Silva, da, A, T., Galisteo Jr., A.J., Lindoso, J.A., Barbosa, L.R., Tempone, A.G., 2017. Nanoliposomal buparvaquone immunomodulates leishmania infantum-infected macrophages and is highly effective in a murine model. Antimicrob. Agents Chemother. 61 https://dx.doi.org/10.1128%2FAAC.02297-16.

Croft, S.S., Hogg, J., Gutteridge, W.E., Hudson, A.T., Randall, A.W., 1992. The activity of hydroxynaphthoquinones against Leishmania donovani. J. Antimicrob. Chemother. 827–832. https://doi.org/10.1093/jac/30.6.827.

Das, S., Ng, W.K., Tan, R.B.H., 2012. Are nanostructured lipid carriers (NLCs) better than solid lipid nanoparticles (SLNs): development, characterizations and comparative evaluations of clotrimazole-loaded SLNs and NLCs? Eur. J. Pharm. Sci. 47, 139–151. https://doi.org/10.1016/j.ejps.2012.05.010.

Date, A.A., Vador, N., Jagtap, A., Nagarsenker, M.S., 2011. Lipid nanocarriers (GeluPearl) containing amphiphilic lipid Gelucire 50/13 as a novel stabilizer: fabrication, characterization and evaluation for oral drug delivery. Nanotechnology 22, 275102 https://doi.org/10.1088/0957-4484/22/27/275102.

Date, T., Paul, K., Singh, N., Jain, S., 2019. Drug-lipid conjugates for enhanced oral drug delivery. AAPS PharmSciTech 20, 41. https://doi.org/10.1208/s12249-018-1272-0.

de Souza, A., Marins, D.S.S., Mathias, S.L., Monteiro, L.M., Yukuyama, M.N., Scarim, C. B., Löbenberg, R., Bou-Chacra, N.A., 2021. Promising nanotherapy in treating leishmaniasis. Int. J. Pharm. 547, 421–431. https://doi.org/10.1016/j.ijpharm.2018.06.018.

Dorlo, T.P.C., van Thiel, P.P.A.M., Huitema, A.D.R., Keizer, R.J., de Vries, H.J.C., Beijnen, J.H., de Vries, P.J., 2008. Pharmacokinetics of Miltefosine in Old World Cutaneous Leishmaniasis Patients. J. Antimicrob. Chemother. 52, 2855–2860. https://doi.org/10.1128/2FAAC.00014-08.

Dorlo, T.P.C., Balasegaran, M., Beijnen, J.H., de Vries, P.J., 2012. Miltefosine: a review of its pharmacology and therapeutic efficacy in the treatment of leishmaniasis. J. Antimicrob. Chemother. 67, 2576–2597. https://doi.org/10.1093/jac/dks275.

Fortin, A., Hendrickx, S., Yardley, V., Cos, P., Jansen, H., Maes, L., 2012. Efficacy and tolerability of oleylphosphocholine (OlPC) in a laboratory model of visceral leishmaniasis. J. Antimicrob. Chemother. 67, 2707–2712. https://doi.org/10.1093/jac/dks273.

Gordillo-Galeano, A., Mora-Huertas, C.E., 2018. Solid lipid nanoparticles and nanostructured lipid carriers: a review emphasizing on particle structure and drug release. Eur. J. Pharm. Biopharm. 133, 285–308. https://doi.org/10.1016/j.ejpb.2018.10.017.

HEALTH, W. ORGANIZATION, 2017. Global Leishmaniasis Update, 2006–2015: a Turning Point In Leishmaniasis Surveillance. World Health Organization, pp. 557–565. https://pubmed.ncbi.nlm.nih.gov/28945057/.

Hendrickx, S., Mondelaers, A., Eberhardt, E., Delputte, P., Cos, P., Maes, L., 2015. In Vivo Selection of Paromomycin and Miltefosine Resistance in Leishmania donovani and L. infantum in a Syrian Hamster Model. Antimicrob. Agents Chemother. 59 https://doi.org/10.1128/AAC.00707-15.

Jain, A., Ran, Y., Yalkowsky, S.H., 2004. Effect of pH-sodium lauryl sulfate combination on solubilization of PG-300995 (an anti-HIV agent): a technical note. AAPS PharmSciTech 5, e45. https://doi.org/10.1208/pt050345.

Jiménez-Antón, M.D., Grau, M., Olías-Molero, A.I., Alunda, J.M., 2019. Syrian hamster as na advanced experimental model for visceral leishmaniasis. Methods Mol. Biol. 1971, 303–314. https://doi.org/10.1007/978-1-4939-9210-2_17.

Jogia, H., Sola, S.P., Garg, L.K., Arutla, S., Reddy, A.M., Venkateswarlu, V., 2014. A Simple, Safe, and Environmentally Friendly Method of FaSSIF and FeSSIF Preparation Without Methylene Chloride. Dissolut. Technol. 45–48. http://dissolutiontech.com/DTresour/201402Articles/DT201402_A05.pdf.

Kobets, T., Grekov, I., Lipoldova, M., 2012. Leishmaniasis: prevention, parasite detection and treatment. Curr. Med. Chem. 19, 1443–1474. https://doi.org/10.2174/092986712799828300.

Korani, S., Korani, M., Bahrami, S., Johnston, T.P., Butler, A.E., Banach, M., Sahebkar, A., 2019. Application of nanotechnology to improve the therapeutic benefits of statins. Drug Discov. Today 24, 567–574. https://doi.org/10.1016/j.drudis.2018.09.023.

Lowe, M.E., Whitcomb, D.C., 2015. Next Generation of Pancreatic Enzyme Replacement Therapy: recombinant Microbial Enzymes and Finding the Perfect Lipase. Gastroenterology 149, 1678–1681. https://doi.org/10.1053/j.gastro.2015.10.025.

Meira, C.S., Gedamu, L., 2019. Protective or detrimental? Understanding the role of host immunity in leishmaniasis. Microorganisms 7, 695. https://doi.org/10.3390/2Fmicroorganisms7120695.

Melby, P.C., Chandrasekar, B., Zhao, W., Coe, J.E., 2001. The hamster as a model of human visceral leishmaniasis: progressive disease and impaired generation of nitric oxide in the face of a prominent Th1-like cytokine response. J. Immunol. 166, 1912–1920. https://doi.org/10.4049/jimmunol.166.3.1912.

Melo, G.D., Goyard, S., Lecoeur, H., Rouault, E., Pescher, P., Fiette, L., Boissonnas, A., Minoprio, P., Lang, T., 2017. New insights into experimental visceral leishmaniasis: real-time *in vivo* imaging of Leishmania donovani virulence. PLoS Negl. Trop. Dis. 11, e0005924 https://doi.org/10.1371/journal.pntd.0005924.

Michel, G., Pomares, C., Ferrua, B., Marty, P., 2011. Importance of worldwide asymptomatic carriers of Leishmania infantum (L. chagasi) in human. Acta Trop. 119, 69–75. https://doi.org/10.1016/j.actatropica.2011.05.012.

Minekus, M., Alminger, M., Alvito, P., Ballance, S., Bohn, T., Bourlieu, C., Carrière, F., Boutrou, R., Corredig, M., Dupont, D., Dufour, C., Egger, L., Golding, M., Karakaya, S., Kirkhus, B., Le Feunteun, S., Lesmes, U., Macierzanka, A., Mackie, A., Marze, S., McClements, D.J., Ménard, O., Recio, I., Santos, C.N., Singh, R.P., Vegarud, G.E., Wickham, M.S., Weitschies, W., Brodkorb, A., 2014. A standardised static *in vitro* digestion method suitable for food - an international consensus. Food Funct. 5, 1113–1124. https://doi.org/10.1039/C3FO60702J.

Monteiro, L.M., Löbenberg, R., Cotrim, P.C., Barros de Araujo, G.L., Bou-Chacra, N., 2017a. Buparvaquone Nanostructured Lipid Carrier: development of an Affordable Delivery System for the Treatment of Leishmaniases. Biomed. Res. Int., 9781603, 2017https://doi.org/10.1155/2017/9781603.

Monteiro, L.M., Löbenberg, R., Ferreira, E.I., Cotrim, P.C., Kanashiro, E., Rocha, M., Chung, M.C., Bou-Chacra, N., 2017b. Targeting Leishmania amazonensis amastigotes through macrophage internalisation of a hydroxymethylnitrofurazone nanostructured polymeric system. Int. J. Antimicrob. Agents 50, 88–92. https://doi.org/10.1016/j.ijantimicag.2017.01.033.

Murray, H.W., 2001. Tissue granuloma structure-function in experimental visceral leishmaniasis. Int. J. Exp. Pathol. 82, 249–267. https://doi.org/10.1046/j.1365-2613.2001.00199.x.

Park, S.J., Garcia, C.V., Shin, G.H., Kim, J.T., 2017. Development of nanostructured lipid carriers for the encapsulation and controlled release of vitamin D3. Food Chem. 225, 213–219. https://doi.org/10.1016/j.foodchem.2017.01.015.

Reimão, J.Q., Colombo, F.A., Pereira-Chioccola, V.L., Tempone, A.G., 2012. Effectiveness of liposomal buparvaquone in an experimental hamster model of Leishmania (L.) infantum chagasi. Exp. Parasitol. 130, 195–199. https://doi.org/10.1016/j.exppara.2012.01.010.

Reimão, J.Q., Pita, Pedro, D.P.P., Coelho, A.C., 2020. The preclinical discovery and development of oral miltefosine for the treatment of visceral leishmaniasis: a case history. Exp. Opin. Drug Discov. 15, 647–658. https://doi.org/10.1080/17460441.2020.1743674.

Savić, V., Ilić, T., Nikolić, I., Marković, B., Čalija, B., Cekić, N., Savić, S., 2019. Tacrolimus-loaded lecithin-based nanostructured lipid carrier and nanoemulsion with propylene glycol monocaprylate as a liquid lipid: formulation characterization and assessment of dermal delivery compared to referent ointment. Int. J. Pharm. 569, 118624 https://doi.org/10.1016/j.ijpharm.2019.118624.

Shrivastava, S., Gidwani, B., Kaur, C.D., 2020. Development of mebendazole loaded nanostructured lipid carriers for lymphatic targeting: optimization, characterization, in-vitro and in-vivo evalutation. Part. Sci. Technol. 39, 1–11. https://doi.org/10.1080/02726351.2020.1750515.

Smith, L., Serrano, D.R., Mauger, M., Bolás-Fernández, F., Dea-Ayuela, M.A., Lalatsa, A., 2018. Orally bioavailable and effective buparvaquone lipid-based nanomedicines for visceral leishmaniasis. Mol. Pharm. 15, 2570–2583. https://doi.org/10.1021/acs.molpharmaceut.8b00097.

Souto, E.B., Baldim, I., Oliveira, W.P., Rao, R., Yadav, N., Gama, F.M., Mahant, S., 2020. SLN and NLC for topical, dermal, and transdermal drug delivery. Expert Opin. Drug Deliv. 17, 357–377. https://doi.org/10.1080/17425247.2020.1727883.

Stetefeld, J., McKenna, S.A., Patel, T.R., 2016. Dynamic light scattering: a practical guide and applications in biomedical sciences. Biophys. Rev. 8, 409–427. https://doi.org/10.1007/s12551-016-0218-6.

Sunyoto, T., Potet, J., Boelaert, M., 2018. Why miltefosine – a life-saving drug for leishmaniasis – is unavailable to people who need it the most. BMJ Glob. Health 3, e000709 https://doi.org/10.1136/bmjgh-2018-000709.

Sznitowska, M., Wolska, E., Baranska, H., Cal, K., Pietkiewicz, J., 2017. The effect of a lipid composition and a surfactant on the characteristics of the solid lipid microspheres and nanospheres (SLM and SLN). Eur. J. Pharm. Biopharm. 110, 24–30. https://doi.org/10.1016/j.ejpb.2016.10.023.

Teeranachaideekul, V., Boonme, P., Souto, E.B., Müller, R.H., 2008. Junyaprasert, V. B. Influence of oil content on physicochemical properties and skin distribution of Nile red-loaded NLC. J. Control. Release 128, 134–141. https://doi.org/10.1016/j.jconrel.2008.02.011.

Thapa, R., Mondal, S., Riikonen, J., Rantanen, J., Näkki, S., Nissinen, T., Närvänen, A., Lehto, V.P., 2021. Biogenic nanoporous silicon carrier improves the efficacy of buparvaquone against resistant visceral leishmaniasis. PLoS Negl. Trop. Dis.. 15, e0009533. https://doi.org/10.1371/journal.pntd.0009533.

Thomaidou, E., Horev, L., Jotkowitz, D., Zamir, M., Ingber, A., Enk, C.D., Molho-Pessach, V., 2015. Lymphatic dissemination in cutaneous leishmaniasis following local treatment. Am. J. Trop. Med. Hyg. 93, 770–773. https://doi.org/10.4269/ajtmh.14-0787.

Torcello-Gómez, A., Foster, T.J., 2014. Interactions between cellulose ethers and a bile salt in the control of lipid digestion of lipid-based systems. Carbohydr. Polym. 113, 53–61. https://doi.org/10.1016/j.carbpol.2014.06.070.

Tran, P., Pyo, Y.C., Kim, D.H., Lee, S.E., Kim, J.K., Park, J.S., 2019. Overview of the manufacturing methods of solid dispersion technology for improving the solubility of poorly water-soluble drugs and application to anticancer drugs. Pharmaceutics 11, 132. https://doi.org/10.3390/pharmaceutics11030132.

United States Phamacopoeia, 2019. USP, Dissolution Methods Database. http://www.usp.org/resources/dissolution-methods-database.

Üstündağ-Okur, N., Yurdasiper, A., Gündoğdu, E., Gökçe, E.H., 2016. Modification of solid lipid nanoparticles loaded with nebivolol hydrochloride for improvement of oral bioavailability in treatment of hypertension: polyethylene glycol *versus* chitosan oligosaccharide lactate. J. Microencapsul. 33, 30–42. https://doi.org/10.3109/02652048.2015.1094532.

Vexenat, J.A., Croft, S.L., Campos, Furtado, J, H., Miles, M.A., 1998. Failure of buparvaquone (Butalex) in the treatment of canine visceral leishmaniosis. Vet. Parasitol. 77, 71–73. https://doi.org/10.1016/S0304-4017(96)01150-8.

Vishwakarma, N., Jain, A., Sharma, R., Mody, N., Vyas, S., Vyas, S.P., 2019. Lipid-Based Nanocarriers for Lymphatic Transportation. AAPS PharmSciTech 20, 83. https://doi.org/10.1208/s12249-019-1293-3.

Witayaudom, P., Klinkesorn, U., 2017. Effect of surfactant concentration and solidification temperature on the characteristics and stability of nanostructured lipid carrier (NLC) prepared from rambutan (Nephelium lappaceum L.) kernel fat. J. Colloid Interface Sci. 505, 1082–1092. https://doi.org/10.1016/j.jcis.2017.07.008.

Wu, G., Majewski, J., Ege, C., Kjaer, K., Weygand, M.J., Lee, K.Y., 2004. Lipid corralling and poloxamer squeeze-out in membranes. Phys. Rev. Lett. 93, 028101 https://doi.org/10.1103/PhysRevLett.93.028101.

Zoubari, G., Staufenbiel, S., Volz, P., Alexiev, U., Bodmeier, R., 2017. 110. Effect of drug solubility and lipid carrier on drug release from lipid nanoparticles for dermal delivery. Eur. J. Pharm. Biopharm. 110, 39–46. https://doi.org/10.1016/j.ejpb.2016.10.021.